Biped Robot "ROTTO": Stiff and Compliant

A. Melnykov, F.Palis, A. Rudskyy, M. Konyev and RobotsLab Team
Otto-von-Guericke-University Magdeburg, FEIT/IESY/RobotsLab, 39106, Magdeburg
andriy.melnykov@yahoo.de, Frank.Palis@e-technik.uni-magdeburg.de, tema13tema@yahoo.de, Mykhaylo.Konyev@gmx.net

***Abstract*—The paper deals with designing and developing a biped robot for research purposes. Robot's mechanical structure and drives system are described hereunder in details. Moreover the new modified actuator is discussed. An industrial Ethernet-based real-time communication protocol is introduced and the communication ability between the robot-side hardware and PC-side control system is investigated.**

I. Introduction

During the last years many researchers are engaged in tasks how to develop the efficient robot prototypes and their control system. The paper deals with designing and developing a stiff as well as compliant biped robot based on experience of the RobotsLab group. Moreover, flexible communication bridge for real-time communication between the real control system and real robot is presented. The RobotsLab group is a team of young researchers at the University of Magdeburg. Scientific interests of the group are in the area of robotic, especially in such fields as intelligent and adaptive motion control, optimization and adaption of mechanic and electronic construction of complex mechanisms with many degrees of freedoms, planning complex robot tasks and motion trajectory and so on.

II. Biped robot "ROTTO"

A. Mechanical construction of biped robot "ROTTO"

The main purpose of biped robot constructions is to develop mobile robot able to solve following research tasks:

- research and investigation of low-cost energy gaits (ballistic walking is one of the possible gaits),
- development and research of the methods of force/impedance control of robot foots during contact with the ground,
- investigation of dynamical walking and methods of robot's body stabilization during walking.

To perform above mentioned requirements a biped robot "ROTTO" (see Figures 1 and 2) has been designed and constructed. The kinematical construction of the robot is shown in Figure 2. The robot has been constructed to provide more than 15 Degree Of Freedom (DOF) similar to what human being provides. Suggested robot's construction is characterized by modular structure using linear drive systems in each joint. Bearing structures of the robot are fabricated from carbon material and connected to each other with optimized milled-out aluminum constructions. The aluminum-carbon construction reduces the weight of robot and, at the same time provides sufficient robustness.

The construction of the "hip's" and the "ankle's" joints are implemented in parallel kinematic. Two linear drives actuate the corresponding 2-DOF using the connecting rods and the ball joint. The synchronous and the asynchronous motions of the drives produce the corresponding motion relative to one or another DOF in the joint. It should be pointed out, that such construction ensures the double rotation moment on the two rotation axis.

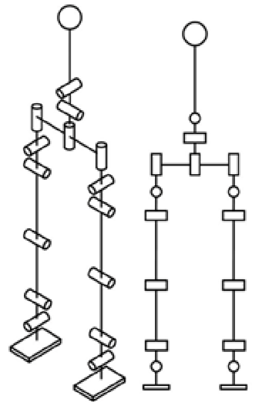

Figure 1. Kinematic structure of biped robot "ROTTO".

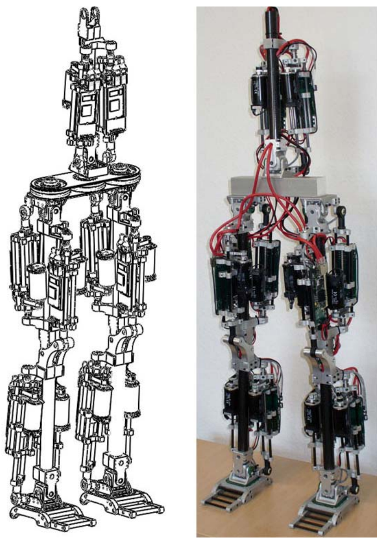

Figure 2. CAD construction (left); real biped robot "ROTTO" (right).

B. Actuators of biped robot "ROTTO"

The actuators of the biped robot "ROTTO" are implemented as linear drives (Figure 3). The brushless EC-motor drives the ball screw using belt transmission with a reduction ratio of two. The linear motion of the ball screw's nut is realized by carbon sticks which are at the same time the direction guide. There is an incremental position sensor on the motor axis. For safety purpose, two limit switches are installed. The on-board electronics collect all the data from sensors and accomplish current control of the EC-motor. The nominal force of this actuator is 128 N with a nominal speed of 0,64 m/s, but the maximal force is 400 N and the maximal velocity is 0,72 m/s. It should be pointed out, that the maximal values of the actuator force and speed can't be reached at the same time.

The complete integration in one module of the motor, the gear, the sensors and the electronic offers the following advantages:

- reduced volume of actuator;
- better dynamic properties;
- higher power density;
- better efficiency;
- the EC-motor and the modular structure of drive provides better reliability as well as integrated diagnose and observation functionality.

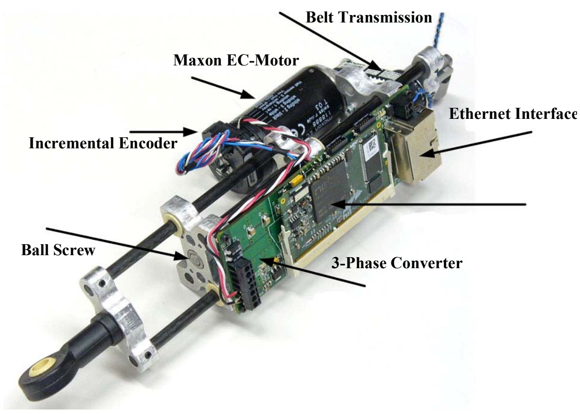

Figure 3. Linear actuator of biped robot "ROTTO".

C. *Modified actuators of biped robot "ROTTO"*

The developed design of the elastic element, combined with the force sensor is shown in Figure 4. Modern composite materials allow a higher energy storage density in the elastic element by smaller masses. The main operating element is a flat coal-plastic spring 5. The deformation of the spring is measured by the Hall-sensor 4 placed in the magnetic field of the two neodymium magnets 3. The glass fibre plate 2 and the screw 1 serve to fix the actor.

D. *Sensors of biped robot "ROTTO"*

The sensor system of the robot consists of components that are standard for mobile robots and that makes possible to achieve autonomous robot functions in an environment. It includes:

- absolute magnetic encoder installed in each robot joint;
- incremental position sensor, two current sensors and two limit switches installed in each of the actuator module;
- six-component force sensor mounted in each leg's shank;
- high precision tri-axis inertial sensor installed on the robot body.

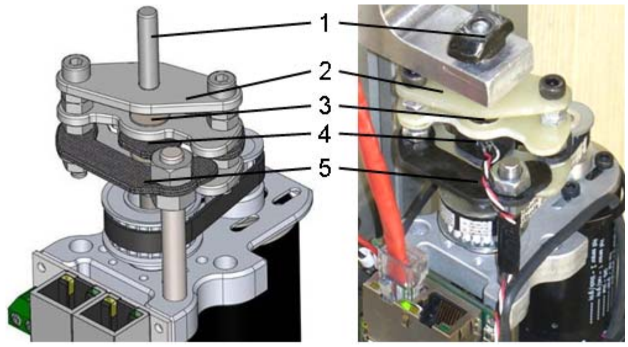

Figure 4. The CAD Model of the elastic actuator (left) and actuator of the robot (right).

Designed foot force sensor provides measurement of forces in wider range in order to comply with the requirements on measurement and control of the support reactions during the dynamical walking. The maximal vertical force is 400N. The maximal values of tangential and lateral forces are chosen up to 300N. The developed sensor is described in [7].

III. HARDWARE CONTROL SYSTEM

The control electronics (Figure 5) as well as the all control architecture and algorithms for the biped robot "ROTTO" have been developed and showed satisfactory results. The control electronic consists of two boards: the small one netX SODIMM module, and the second one with power electronics.

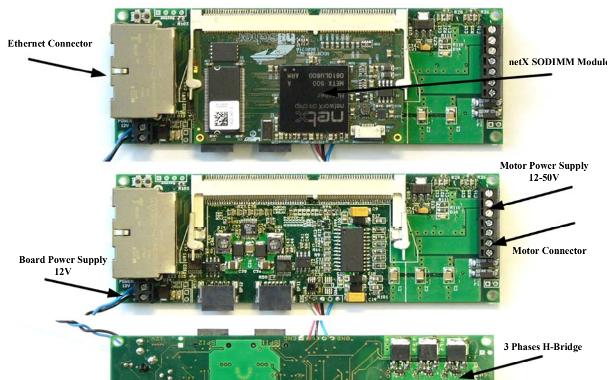

Figure 5. Decentralize control electronics of the biped robot "ROTTO".

Control system with real-time decentralized data gathering and processing builds the kernel of robot system and allows developing of control algorithms with help of hybrid simulation. The implemented control system is already at industry level and is based on typical real-time communication EtherCAT. The developed hardware (see Figure 6) consists of netX communication processor (Hilscher GmbH). The time diagram of communication process is explained in Figure 7. The control system (Control) on Host-PC (xPC Target) is computed each sample time (Tsample) by the information received from the sensors (RD – Receive Data). Computed reference signals of PWM (SD – Send Data) are copied to the EtherCAT packet and the EtherCAT master (CIFx-50) to initialize a telegram (Packet n) transfer. The received data by the EtherCAT slaves (NetX 500) are copied through the DPM (Dual Port Memory) to the xPEC and then to the PWM module. Detailed presentation of decentralize Single-Chip controller based on the netX processor is shown in Figure 8.

The main feature of the EtherCAT communication protocol [5] is the exchange of the data in the loop Master-Slave-Master with one solid telegram. Therefore sending of the response information by the EtherCAT slave is required preliminary preparation of the transfer buffer. The delay $T_{delay} = T_{sample}/2$ between the receipt of the telegram by EtherCAT slave and the monitoring of the sensors is realized. This was done for the minimization of the time difference between monitoring of actual sensors information (ADC, ENC and etc.) and the instant of usage them in the control calculation (n+2 xPC Tact). Received information from sensors (RD) is saved to the transfer buffer of the EtherCAT slave. After that it will be sent in the next closest transfer packet (Packet n+1) and will be actual on the n+2 work period.

The standard PC is used as a control computer (Host PC). Therefore the jitter time (Tjitter) in the communication system due to large number of hardware peripheries is occurred. For the minimization of jitter time the practically all of hardware peripheries are tuned off in the BIOS of PC. The maximal jitter time in our communication system is less than $15\mu s$.

Such communication system allows using of important technique in the robotic area as hybrid simulation technique. Starting with the SiL simulation, where the developed control system in Matlab/Simulink has the possibility to communicate with the real legged robot, the control system has acquired a new level so-called Rapid Control Prototyping.

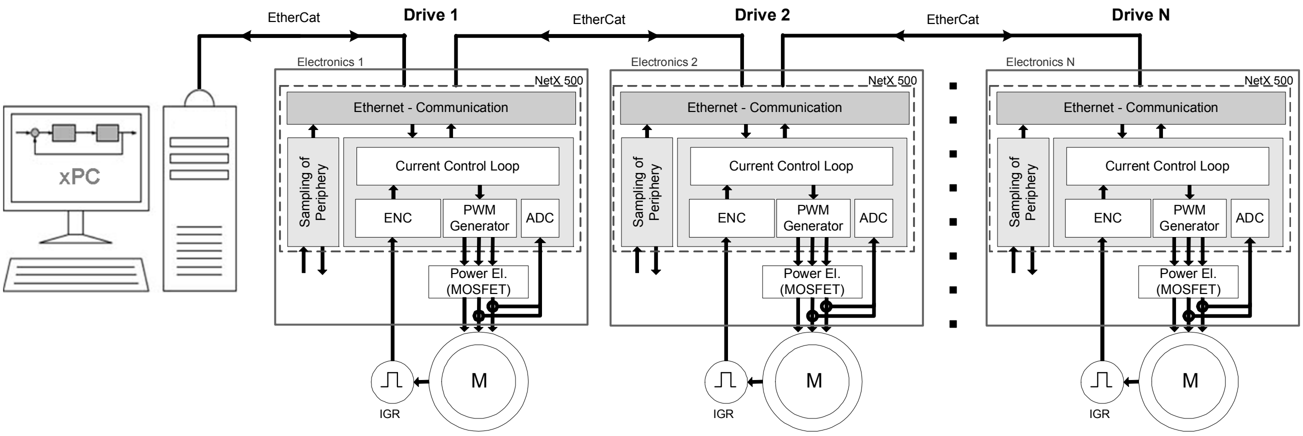

Figure 6. Flexible communication system based on netX processors.

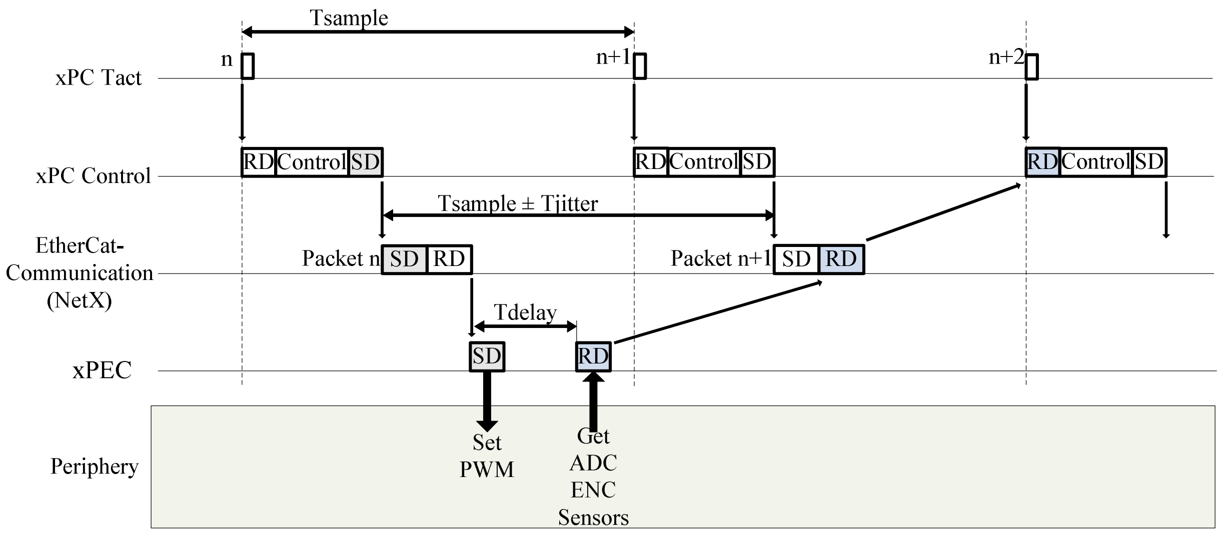

Figure 7. Time diagram of communication process.

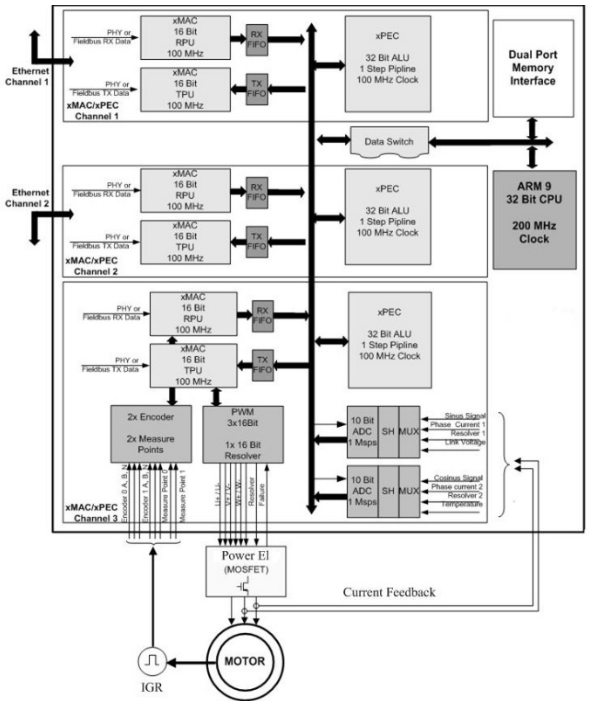

Figure 8. Decentralize Single-Chip controller based on netX processor.

The current control loop is shown in Figure 9. Current control loop is implemented in the netX/xPEC. The current control is calculated synchronously with the PWM module with 28 kHz cycle. The control signal (reference current value) and the sensors signals (motor position, velocity and so on) are exchanged between netX processor and external control PC (with xPC-Target real-time OS) using an EtherCAT communication protocol. Sensors signals are used as the feedback signals for the position/velocity control loops (Figure 10). The sample time of the position/velocity control loops depends on the power of the control PC. In our case (3GHz processor from Intel) the sample time is equal 1ms and can be decrease to 0,5ms.

Phase currents (ia_ist, ib_ist) are measured in the netX by the way of sampling of intern ADC module and are recalculated from coordinate system ABC in coordinate system DQ using Park-Clarke transformation:

$$i_D = \frac{3}{2}\left[i_A \sin(\varphi) + i_B \sin\left(\varphi - \frac{2\pi}{3}\right) + i_C \sin\left(\varphi + \frac{2\pi}{3}\right)\right]$$
$$i_Q = \frac{3}{2}\left[i_A \cos(\varphi) + i_B \cos\left(\varphi - \frac{2\pi}{3}\right) + i_C \cos\left(\varphi + \frac{2\pi}{3}\right)\right] \qquad (1)$$

IV. ACTUATOR CONTROL SYSTEM

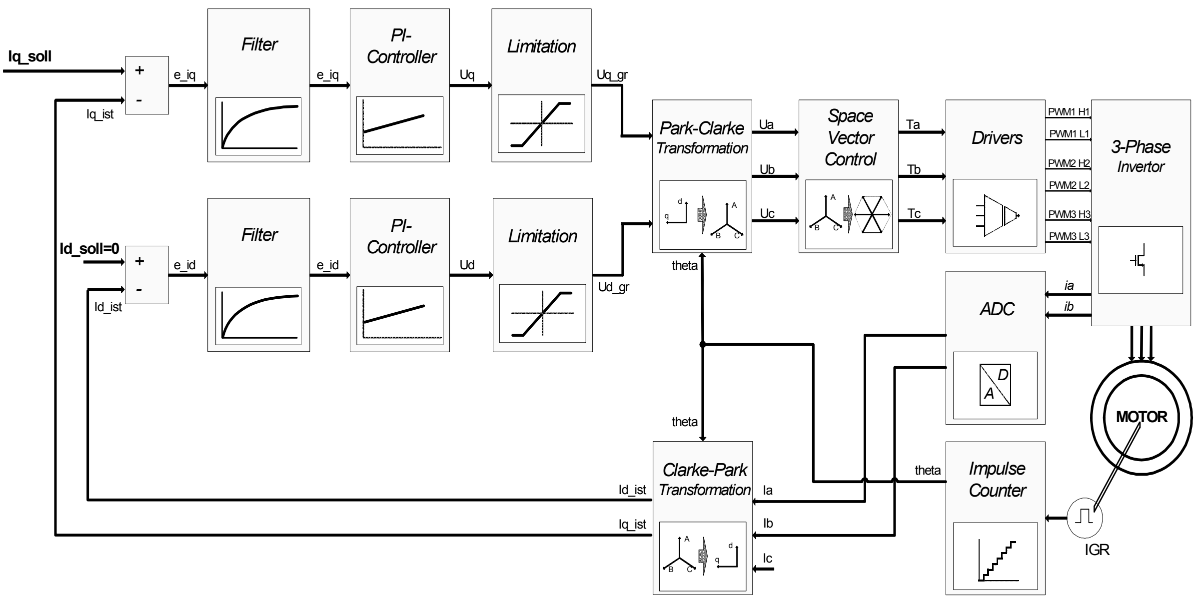

Figure 9. Current control loop in the netX/xPEC.

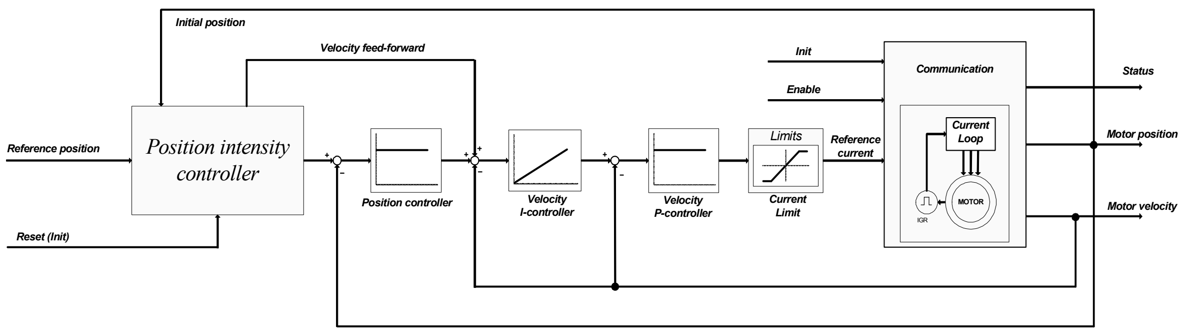

Figure 10. Position/velocity control loops.

The error between reference and real current is controlled by the PI controller:

$$\frac{U}{e_i} = P_{Cont} + I_{Cont} \cdot \frac{1}{1 - z^{-1}} \quad (2)$$

The voltage is transformed from the coordinate system DQ in coordinate system ABC using the inverse Clarke-Parke transformation:

$$\begin{aligned} U_A &= i_D \sin(\varphi) + i_Q \cos(\varphi) \\ U_B &= i_D \sin\left(\varphi - \frac{2\pi}{3}\right) + i_Q \cos\left(\varphi - \frac{2\pi}{3}\right) \\ i_C &= i_D \sin\left(\varphi + \frac{2\pi}{3}\right) + i_Q \cos\left(\varphi + \frac{2\pi}{3}\right) \end{aligned} \quad (3)$$

A. Velocity/Position control loops

The velocity and position control loops are developed in Matlab/Simulink and are compiled to the control PC using Real-Time-Workshop-Tools [4]. The velocity and the position control loops are shown in the Figure 8.

The accuracy and the correctness of the Permanent Magnet Synchronous Motor (PMSM) control depend on the correct determination of the rotor position. Therefore following algorithm has been developed to determine the exact position of the rotor:

1. reference currents are id_ref = 5A, iq_ref = 0A for rotor positioning along the flux axis D;
2. one second pause for the exact positioning;
3. reset of the IGR's counter;
4. start the current loop, in other words wait for the reference value of iq_ref, the reference value of id_ref is equal 0A.

To ensure correct working of the position control loop when a step reference signals is applied a second order position intensity controller (Figure 11) has been developed.

The experimental results of position/velocity control loops as well as current control loop are shown in Figure 12. Experiments have been carried out on the linear drive without any loads. The position reference signal has been applied as the step signal.

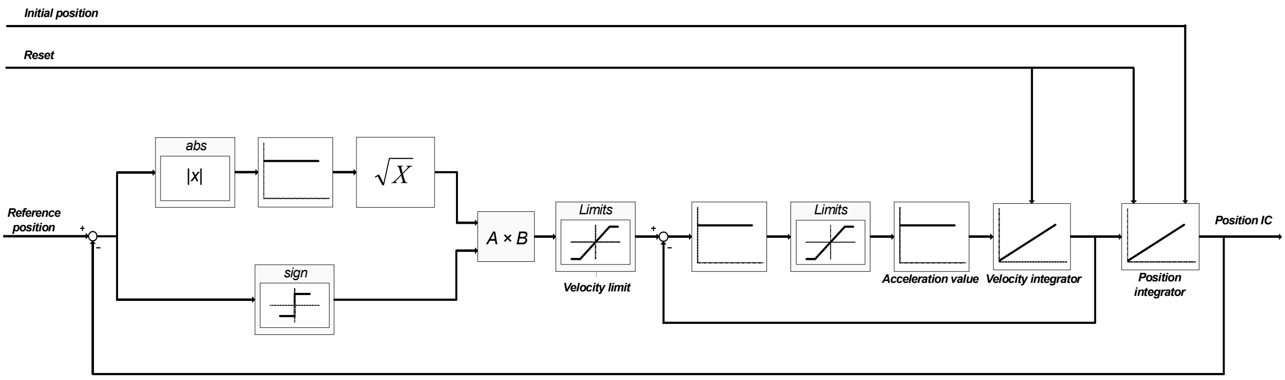

Figure 11. Position intensity controller.

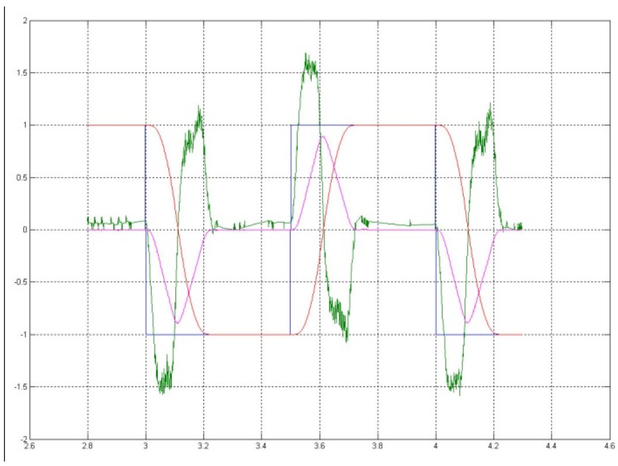

Figure 12. Experimental results: blue – reference position (±10 revolutions); red – actual position (±10 revolutions); magenta – velocity (±13000 rpm); green – current (±3,6A).

B. Force/Position control loops of modified actor

The structure of the force control system is shown in Figure 13.

The force control system has a subordinate structure. There is only one inner control loop – the current control loop. Such approach allows reaching the highest dynamical characteristics of the force control loop. Some successful attempts of using such structure are shown in the works of MIT-University [3].

The force control loop is controlled by the PD-regulator. The dotted feedbacks in Figure 14 are not taken into account when designing the PD-controller. This neglect can be made because of the high dynamics of the force control circuit. These feedbacks are considered as a disturbances and don't cause any instabilities in the system. The step response of the force control loop is shown in Figure 15. The first sequence is 15 ms by the bandwidth of the force control loop of 50 Hz.

The position control system is shown in Figure 16. The above considered force control loop is the inner loop of the position control system.

The coefficient K_D determines the system damping. The coefficient K_P and the value F_G are the most interesting because their variation allows the achieving the specific properties of the position control system when getting into contact with environment. For example, by setting a small value of coefficient K_P the behaviour of the system in contact is elastic (low impedance, artificial spring). Another task – a precise position control with force saturation in the contact point – can be achieved by setting of higher value of coefficient K_P and a given value of F_G. Such case is illustrated in Figure 17, where the end-position is not reached as a result of an impact with an obstacle.

V. CONCLUSION

For the humanoid robot ROTTO an intelligent decentralized linear drive system was developed. It consists of velocity and position controlled brushless EC-motor with ball screw and belt transmission. Force sensors allow the implementation of a force/position control loop. Due to this feature mechanical impedance can be controlled in a wide range.

REFERENCES

[1] http://www.uni-magdeburg.de/ieat/robotslab

[2] http://www.hilscher.com Hilscher GmbH, Hattersheim, Germany

[3] http://www.ai.mit.edu/projects/leglab, MIT Leg Lab, Stand 2008

[4] http://www.mathworks.com/products/rtwembedded

[5] Konyev, Palis, Schmucker, Zavgorodniy, Telesh, Rusin, Rudskiy, Melnikov. Walking robot "Anton": design, simulation, experiments. 11th Int. Conference on CLAWAR, 08-10 September 2008, Coimbra

[6] Palis, Dzhantimirov, Schmucker, Zavgorodniy, Telesh. HIL/SIL by development of six-legged robot SLAIR 2. 10th Int. Conference on CLAWAR, 16-18 July 2007, Singapore

[7] Konyev, Palis, Schmucker, Zavgorodniy, Telesh, Melnykov, Rudskyy. Presentation of a new biped robot "ROTTO". 12th Int. Conference on CLAWAR, 9-11 September 2009, Istanbul

[8] Pratt J., Williamson, Dillworth, Pratt G., Ulland, Wright. Stiffness Isn't Everything. Proceedings of the 4th International Symposium on Experimental Robotics (ISER'95, USA, California, Stanford, July 1995)

[9] Pratt J., Torres, Dilworth, Pratt, G. Virtual Actuator Control. Proceedings of the IEEE International Conference on Intelligent Robots and Systems (IROS '96, Osaka, Japan, 1996)

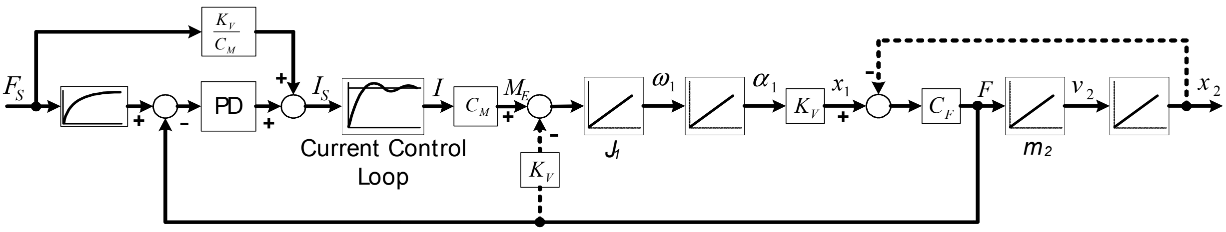

Figure 13. Structural scheme of the force control system, where CF – the coefficient of the spring rigidity (spring constant), KV – coefficient of the conversion of the rotational motion into the translational motion, CM – coefficient of the conversion from current to mechanical torque.

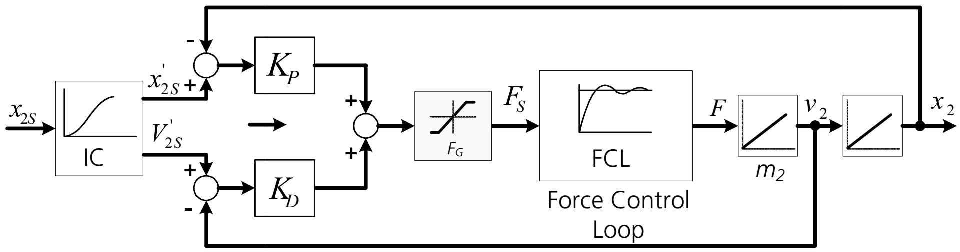

Figure 14. The position control loop.

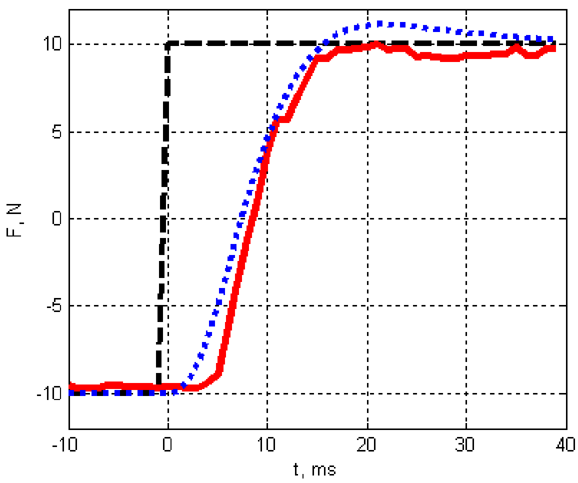

Figure 15. Step response of the force control loop: dotted line – modelling; solid line – experiment.

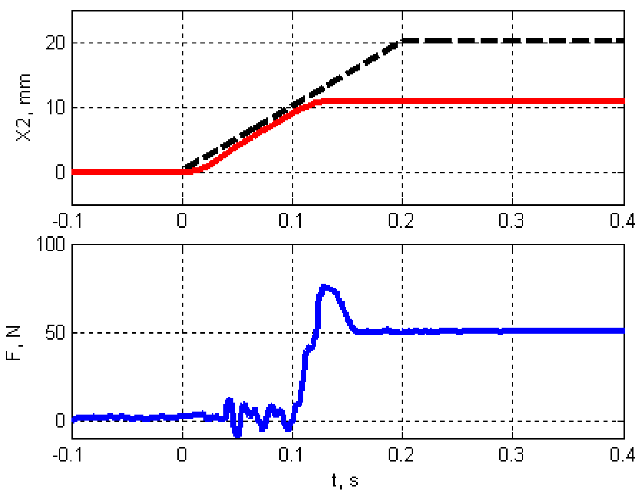

Figure 16. Impact with an obstacle by position control: dotted line – desired position; red line – actual position; blue line – force in the contact.